Real-Time Cavity QED with Single Atoms

C. J. Hood, M. S. Chapman, * T. W. Lynn, and H. J. Kimble

Norman Bridge Laboratory of Physics 12-33, California Institute of Technology, Pasadena, California 91125
(Received 18 November 1997)

The combination of cold atoms and large coherent coupling enables investigations in a new regime in cavity QED with single-atom trajectories monitored in real time with high signal-to-noise ratio. The underlying "vacuum-Rabi" splitting is clearly reflected in the frequency dependence of atomic transit signals recorded atom by atom, with evidence for mechanical light forces for intracavity photon number <1. The nonlinear optical response of one atom in a cavity is observed to be in accord with the one-atom quantum theory but at variance with semiclassical predictions. [S0031-9007(98)06037-2]

An important trend in modern physics has been the increasing ability to isolate and manipulate the dynamical processes of individual quantum systems, with interactions studied quantum by quantum. In optical physics, examples include cavity QED with single atoms and photons [1] and trapped ions cooled to the motional zero point [2], while in condensed matter physics, an example is the Coulomb blockade with discrete electron energies [3]. An essential ingredient in these endeavors is that the components of a complex quantum system should interact in a controlled fashion with minimal decoherence. More quantitatively, if the off-diagonal elements of the system's interaction Hamiltonian are characterized by $\langle H_{\text{int}} \rangle \sim \hbar g$, where g is the rate of coherent, reversible evolution, then a necessary requirement is to achieve *strong coupling* for which $g > \beta \equiv \max[\Gamma, T^{-1}]$ with T as the interaction time and Γ as the set of decoherence rates for the system.

Although there are many facets to investigations of such open quantum systems, our primary motivation has been to exploit strong coupling in cavity QED to enable research in quantum measurement and more generally, in the emerging field of quantum information dynamics [4]. Several experiments in cavity QED have investigated the nonperturbative interaction of an atom with the electromagnetic field at the level of a single photon; for this system $2g_0$ is the single-photon Rabi frequency and $\Gamma \equiv \{\gamma_\perp, \kappa\}$, with $\gamma_\perp$ as the atomic dipole decay rate and κ as the rate of decay of the cavity field [5–8]. However, without exception these experiments have employed atomic beams in settings for which the information per atomic transit (of duration T) is $I \equiv \frac{g_0^2 T}{\beta} \sim 1$, so that measurements over an ensemble of atoms are required. For example, the passage of a Rydberg atom through a microwave cavity and its subsequent measurement provides a single bit of information [5,7].

By contrast, an exciting recent development in cavity QED has been the ability to observe single-atom trajectories in *real time* with $I \gg 1$ [9]. In this method the transmitted power of a probe beam is monitored as cold atoms fall between the mirrors of a high-finesse optical resonator, with the probe transmission significantly altered by the position-dependent interaction between atom and cavity field [10,11].

Similarly enabled by the use of cold atoms, the research reported in this Letter exploits the largest coupling g_0 achieved to date to explore a new regime in cavity QED, for which single-atom trajectories directly reveal the nature of the underlying one-atom master equation. More specifically, for atoms taken one by one, we map the frequency response of the atom-cavity system, and thereby directly determine g_0 from the vacuum-Rabi splitting. For probe excitation near the coincident atom-cavity resonance, the nonlinear saturation behavior of the atom-cavity system is found to be in accord with the single-atom master equation but at variance with semiclassical theory. However, for probe detunings $\Delta \sim \pm g_0$, we observe a marked asymmetry in the vacuum-Rabi spectrum; few trajectories achieve optimal coupling with a blue detuned probe, an effect which we attribute to light forces even for photon numbers <1. Notably, this is the first experiment for which the interaction energy $\hbar g_0$ is greater than the atomic kinetic energy.

Our apparatus is shown schematically in Fig. 1. The Fabry-Perot cavity consists of two superpolished spherical mirrors of radius of curvature 10 cm, forming a cavity of length 10.1 μm and finesse $\mathcal{F} = 1.8 \times 10^5$. In this cavity $(g_0, \kappa, \gamma_\perp, T^{-1})/2\pi = (120, 40, 2.6, 0.002)$ MHz, where the atom-field coupling coefficient g_0 is determined by the cavity geometry (and the known transition dipole moment [12]), κ is the measured linewidth of the TEM$_{00}$ mode of the cavity, $\gamma_\perp$ is the dipole decay
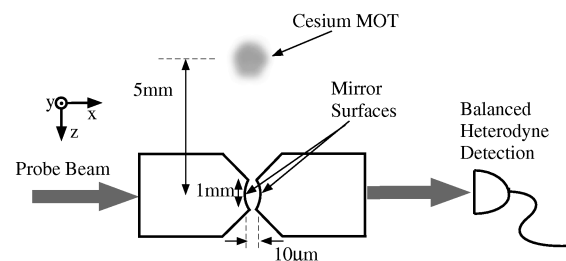
FIG. 1. Schematic of the experimental apparatus.

rate for the Cs $(6S_{1/2}, F = 4, m_F = 4) \rightarrow (6P_{3/2}, F = 5, m_F = 5)$ transition ($\lambda = 852.36$ nm) [12], and typical transit times for atoms through the cavity mode (waist $w_0 \simeq 15$ μm) are $T \simeq 75$ μs. These rates correspond to critical photon and atom numbers ($m_0 \equiv \gamma_\perp^2/2g_0^2, N_0 \equiv 2\kappa\gamma_\perp/g_0^2) = (2.3 \times 10^{-4}, 0.015)$, and to optical information per atomic transit $I \sim 5.4 \times 10^4 \pi$ [4]. The probe transmission (typical power 10 pW) is measured using balanced heterodyne detection with overall efficiency 40%. The length of the cavity is actively stabilized by chopping an auxiliary locking beam [6].

Our experimental procedure consists of loading the magneto-optical trap (MOT) for 0.5 s, performing sub-Doppler cooling to 20 μK and then dropping the atoms, all the while monitoring transmission of a circularly polarized probe beam with fixed detuning $\Delta \equiv \omega_P - \omega_{AC}$ (where $\omega_{atom} = \omega_{cavity} \equiv \omega_{AC}$) [13]. As an atom falls into the cavity, it encounters a spatially dependent coupling coefficient $g(\vec{r}) \simeq g_0 \cos(2\pi x/\lambda) \exp[-(y^2 + z^2)/w_0^2] \equiv g_0\psi(\vec{r})$. Hence as $g(\vec{r})$ increases from zero, the otherwise coincident atomic and cavity resonances map to a nondegenerate superposition of dressed states for the atom-cavity system, so the probe spectrum evolves from a simple Lorentzian to a "vacuum-Rabi" spectrum with two peaks at $\omega_{AC} \pm g(\vec{r})$, as illustrated in Fig. 2. Displayed is a series of theoretical transmission spectra $\overline{m}(\Delta) \equiv |\langle a \rangle|^2$ associated with the mean intracavity amplitude $\langle a \rangle$ calculated from the steady-state solution of the master equation for a single atom (of infinite mass) placed at sites $\vec{r}_l$ with coupling $g(\vec{r}_l)$ [11]. Of course, the spectrum at $g(\vec{r}) = 0$ is simply the response of the cavity with no atom present, hereafter denoted by $\overline{n}(\Delta) = \overline{n}_0/[1 + (\Delta/\kappa)^2]$, while that at $g(\vec{r}_l) = g_0$ corresponds to an optimally coupled atom.

Although most atoms never reach a region of optimal coupling, some do enter in the desired $m_F = 4$ sublevel

and fall through antinodes of the field; these encounter an increasing $g(\vec{r})$ which sweeps the vacuum-Rabi sidebands outward in frequency to a maximum of $\pm g_0/2\pi = \pm 120$ MHz. The bold traces in Fig. 2 illustrate the corresponding evolution of $\overline{m}$ for three probe detunings Δ relevant to our observations. The process reverses as the atom leaves the cavity.

Turning to our measurements, we present in Fig. 3(a)–3(c) examples of the time-dependent transmission $T(t) \equiv \overline{m}(t)/\overline{n}$ of the atom-cavity system at the probe detunings of Fig. 2. With $\omega_P \approx \omega_{AC}$ [Fig. 3(a)] we observe first decreasing probe transmission [due to increasing $g(\vec{r})$ as the atom enters the mode volume], then a minimum in transmission [when $g(\vec{r}) \approx g_0$], and finally transmission increasing to its original value (as the atom exits the cavity). $T_{min} \approx 10^{-2}$ is regularly observed for single atom transits. Conversely, for $\Delta/2\pi = -120$ MHz $\approx g_0/2\pi$ [Fig. 3(c)], the transmission increases as the atom enters the cavity mode, peaking at $T_{max} \approx 3.5$ when $g(\vec{r}) \approx g_0$, and then falling as the atom exits. Finally, an intermediate regime $\Delta/2\pi = -40$ MHz $\approx \frac{1}{3}g_0/2\pi$ exhibits more complicated behavior [Fig. 3(b)]. Here, as the atom enters the cavity, the transmission first increases as the lower Rabi peak sweeps past ω_P, then decreases to a minimum when $g(\vec{r}) \approx g_0$, and finally passes through a second maximum as $g(\vec{r})$ decreases with the atom's departure [14].

To confirm the qualitative characteristics of the vacuum-Rabi spectrum during a single atom transit we simultaneously record the transmission of two probe beams, as in Figs. 3(d),3(e). For probes with detunings $\Delta_{1,2} \approx \mp g_0$, the cavity transmission increases simultaneously for each

FIG. 2. $\overline{m}(\Delta) \equiv |\langle a \rangle|^2$ as a function of probe detuning Δ for atomic positions $\vec{r}_l$ such that $g(\vec{r}_l) = \{0, g_0/9, \ldots, g_0\}$, with probe intensity fixed at $\overline{n}_0 = 1$. For an atom transiting the cavity, this *position dependent coupling* yields a *time dependent transmission*, indicated by the bold curves for fixed probe detunings $\Delta/2\pi = \{-20, -40, -120\}$ MHz.
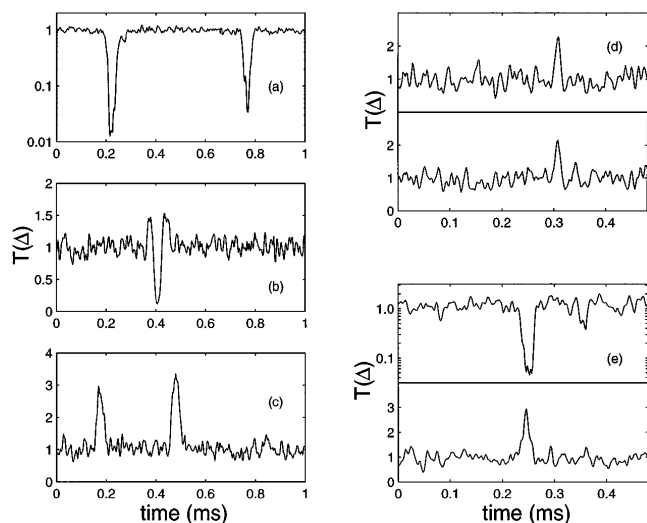
FIG. 3.   Measured cavity transmission $T(t) = \overline{m}(t)/\overline{n}$ as a function of time for individual atom transits. Traces (a)–(c) are for $\Delta/2\pi = \{-20, -40, -120\}$ MHz with $\overline{n}_0 = 0.7, 0.6, 1.0$. (d) $\Delta_{1,2}/2\pi = \{-100, +100\}$ MHz with $\overline{n}_{01,02} = 0.38, 0.22$. (e) $\Delta_{1,2}/2\pi = \{-20, -100\}$ MHz with $\overline{n}_{01,02} = \{0.05, 0.3\}$. All traces are acquired with 100 kHz resolution bandwidth and digitized at 500 kHz sampling rate.

probe during the atom transit [Fig. 3(d)]. For one probe near resonance ($\Delta_1 \approx 0$) and the other red-detuned ($\Delta_2 \approx -g_0$), there is a reduction in the transmission at Δ_1, and an increase in the transmission at Δ_2 [Fig. 3(e)]. Note that the signal-to-noise for these traces is less than that for single-probe measurements due to saturation, reflecting a limitation *in principle* to the rate at which information can be extracted from this quantum system.

We next map the frequency response of the atom-cavity system over a range of detunings $\frac{|\Delta|}{2\pi} \leq 200$ MHz (Fig. 4). Clearly evidenced is a double-peaked structure reminiscent of the "vacuum-Rabi" splitting, with peaks near $\pm g_0/2\pi$, as was first observed in Ref. [15]. In contrast to previous work with atomic beams, here atoms are observed one by one with negligible effect from background atoms in the tails of the cavity-mode function [16] (such "spectator" atoms contribute in aggregate an effective atom number $\overline{N}_e < 0.04$).

At each value of Δ, a series of about 50 trap drops is made, yielding up to 800 single-atom events, from which the maximum and/or minimum relative transmissions, shown in Fig. 4, are determined. Note that at small (large) detunings only decreases (increases) in transmission are observed [cf. Figs. 3(a),3(c)], whereas for detunings 40 MHz $\leq |\Delta|/2\pi \leq 60$ MHz both increases and decreases are observed [cf. Fig. 3(b)], hence both a maximum *and* a minimum transmission are shown. Again, the transit signals are normalized to the transmission of the empty cavity at each frequency to give $T(\Delta)$, with $\overline{n}_0$ varying from ≈ 0.6 photons near resonance to ≈ 1.4 photons at $\Delta/2\pi = \pm 200$ MHz.

One of the most striking features of the data in Fig. 4 is the asymmetry of the spectrum between red and blue probe detunings, both in the magnitude and abundance of transits. Indeed, the number of events observed with $T(\Delta) \approx 2.5$ around $\Delta \approx +g_0$ is 5 times smaller than for $T(\Delta) \approx 3.3$ around $\Delta \approx -g_0$. Residual atom-cavity detunings are insufficient to explain the observed asymmetry (the cavity lock results in $\omega_{\text{atom}} \simeq \omega_{\text{cavity}}$
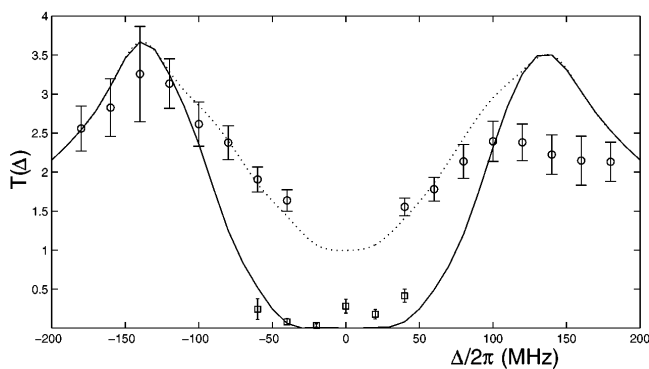
FIG. 4. Maximum ($\bigcirc$) and minimum ($\square$) normalized transmission $T(\Delta)$ versus detuning Δ measured via single atom events. The solid curve gives $T(\Delta)$ for an atom with $g(\vec{r}) = g_0$ (the vacuum-Rabi spectrum), while the dashed line is the maximum transmission for any coupling $g(\vec{r}) \leq g_0$.

with systematic offsets below ± 2 MHz and peak-to-peak excursions less than ± 5 MHz). We attribute this asymmetry to mechanical light forces from the probe beam affecting the atom's trajectory. As analyzed in Ref. [17], weak excitation by a coherent probe tuned to $\Delta_\pm \approx \pm g_0$ gives rise to a pseudopotential (for times $\gg \kappa^{-1} \sim 4$ nsec), with depth $\pm \hbar g_0 p_\pm$, where $p_\pm \propto \overline{m}(\Delta_\pm)$ is the probability of occupation of the upper (lower) dressed state. Since $\hbar g_0/k_B \approx 7$ mK, such light forces can be significant even for $\overline{m} \sim 0.5$ photons. We thus expect significant channeling of atomic trajectories into regions of high light intensity and strong coupling for a red-detuned probe ($\Delta < 0$). Conversely, a blue-detuned probe ($\Delta > 0$) creates a potential barrier and prevents an atom from reaching areas of optimal coupling. Apart from its relevance to the spectrum of Fig. 4, this phenomenon suggests the possibility of trapping single atoms in the cavity mode with single photons.

For comparison with theory, the solid curve in Fig. 4 gives $T(\Delta)$ obtained from the steady-state solution of the master equation for a single stationary atom with $g(\vec{r}) = g_0$. Because the largest increases in transmission for $|\Delta| \gtrsim g_0$ and similarly the deepest downgoing transits near $\Delta = 0$ correspond to atoms with maximal coupling g_0, these data points track the solid curve well. However, for intermediate detunings 40 $\lesssim |\Delta|/2\pi \lesssim 100$ MHz, the maximum observed transmission corresponds to a *smaller* value of coupling, $g(\vec{r}) \simeq |\Delta| < g_0$, and so these points are not expected to fall on the solid curve. We can, however, determine the maximum expected transmission at each Δ by considering all couplings $g(\vec{r}) \leq g_0$, with the result plotted as the dashed curve in Fig. 4. Agreement between this *ideal one-atom* theory and experiment is evident for $\Delta < 0$, providing direct confirmation of the quoted value for g_0.

Note that because $g(\vec{r})$ for most atoms never reaches g_0 as they transit the cavity, we record a continuous distribution of transit sizes at each Δ, from which the maximum and minimum values of $T(\Delta)$ of Fig. 4 and the associated uncertainties are determined as follows. First note that in the absence of mechanical forces, a fraction $f_t(\Delta) \sim 0.1$ of all *detectable* transit signals reach coupling $0.9g_0 \leq g(\vec{r}) \leq g_0$. Further, for data with $\Delta/2\pi = -120$ MHz and $\Delta \sim 0$ (which have the best statistics and highest signal-to-noise ratios), as we vary the fraction f_e of the total data included in the set of optimal events (maxima or minima), both T and the sample standard deviation σ_d are found to be relatively insensitive to the choice of f_e for $f_e \lesssim 0.15$. We thus take $f = 0.15$ to determine the set of transits to be included in Fig. 4 (and hence to fix σ_d from the associated distribution). In addition, there is an uncertainty σ_q arising from the noise of the detected probe beam itself, which is estimated by an appropriate scaling of the noise for "no-atom" data bracketing a given transit signal. The quantity $\sigma = \sqrt{\sigma_d^2 + \sigma_q^2}$ is shown in Fig. 4 to estimate the error in T at each Δ. For all our data,
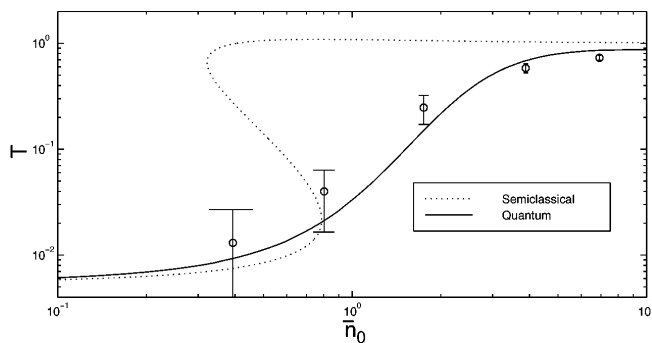
FIG. 5. Transmission T versus probe photon number $\bar{n}_0$ for maximally coupled atom transits for fixed $\Delta/2\pi = -20$ MHz. The solid line results from the quantum master equation for one atom with $g(\vec{r}) = g_0$, while the dashed line is the semiclassical bistability state equation.

the absolute uncertainty in the quoted photon numbers is $\simeq \pm 30\%$.

In a final series of measurements shown in Fig. 5, we explore the nonlinear saturation behavior of the atom-cavity system. We vary $\bar{n}_0$ with the probe beam fixed at detuning $\Delta/2\pi = -20$ MHz. At each $\bar{n}_0$ we again digitize the cavity transmission for a large number of transits, with a set of "optimal" single-atom events determining the value of T and its uncertainty σ. The solid curve of Fig. 5 is from the steady-state solution of the master equation for a single (stationary) atom with $g(\vec{r}) = g_0$, with reasonable agreement between the data and this ideal quantum model. By contrast, the dashed line is the semiclassical transmission function [18] evaluated for the parameters of our experiment, and exhibits bistable behavior. Shifts from the semiclassical bistability curve have also been predicted for other regimes of cavity parameters [19].

In conclusion, by exploiting laser cooled atoms in cavity QED, a unique optical system has been realized which approximates the ideal situation of one atom strongly coupled to a cavity, with $\hbar g$ larger than even the atomic kinetic energy. The system's characteristics have been explored atom by atom, leading to measurements of the "vacuum-Rabi" splitting and of the nonlinear transmission for probe photon number ~ 1. Because $I \gg 1$, the system offers considerable opportunity for long interaction times and controlled quantum dynamics, as in our current efforts to generate a bit stream containing $m \sim 10^4$ photons with a single falling atom [20] as well as to trap one atom in the quantized cavity field. Although the atomic center-of-mass (CM) motion has here been treated classically, this work sets the stage for investigations of quantum dynamics involving the quantized CM and the internal atomic dipole + cavity field degrees of freedom [21,22], including trapping by way of the "well-dressed" states for single quanta [23].

*Permanent address: School of Physics, Georgia Institute of Technology, Atlanta, GA 30332-0430.

[1] *Cavity Quantum Electrodynamics,* edited by P. Berman (Academic Press, San Diego, 1994).

[2] C. Monroe *et al.,* Phys. Rev. Lett. **75**, 4011 (1995).

[3] D. C. Ralph, C. T. Black, and M. Tinkham, Phys. Rev. Lett. **78**, 4087 (1997).

[4] H. J. Kimble, Philos. Trans. R. Soc. London A **355**, 2327 (1997).

[5] G. Rempe, F. Schmidt-Kaler, and H. Walther, Phys. Rev. Lett. **64**, 2783 (1990).

[6] G. Rempe *et al.,* Phys. Rev. Lett. **23**, 1727 (1991).

[7] M. Brune *et al.,* Phys. Rev. Lett. **76**, 1800 (1996).

[8] J. J. Childs *et al.,* Phys. Rev. Lett. **77**, 2901 (1996).

[9] H. Mabuchi *et al.,* Opt. Lett. **21**, 1393 (1996).

[10] G. Rempe, Appl. Phys. B **60**, 233 (1995).

[11] A. C. Doherty *et al.,* Phys. Rev. A **56**, 833 (1997).

[12] C. E. Tanner *et al.,* Nucl. Instrum. Methods Phys. Res., Sect. B **99**, 117 (1995).

[13] The circularly polarized probe beam drives the cycling transition $m_F = 4 \to m_F = 5$ and provides optical pumping to this sublevel as an atom enters the cavity mode. The magnetic field is zeroed at the site of the MOT to allow sub-Doppler cooling and from the coil geometry, should also be well zeroed at the cavity mode. Explicit spatial quantization obtained by switching a magnetic field "on" along the cavity axis as the atom transits produced no significant impact on the transit signals. Note that transit signals from atoms that are incorrectly optically pumped and driven on transitions other than $mF = 4 \to m_F = 5$ are eliminated by our selection of optimal events.

[14] The transit signals of Fig. 3 are smoothly varying without the rapid oscillations recorded in Ref. [9], which were tentatively attributed to motion along the standing wave. Here we suspect that the tenfold increase in g leads to mechanical forces which inhibit this motion.

[15] R. J. Thompson, G. Rempe, and H. J. Kimble, Phys. Rev. Lett. **68**, 1132 (1992).

[16] Q. Turchette *et al.,* Phys. Rev. A (to be published).

[17] A. S. Parkins (unpublished); P. Horak *et al.,* Phys. Rev. Lett. (to be published).

[18] L. A. Lugiato, *Progress in Optics,* edited by E. Wolf (Elsevier Science Publishers, Amsterdam, 1984), Vol. XXI.

[19] C. M. Savage and H. J. Carmichael, IEEE J. Quantum Electron. **24**, 1495 (1988).

[20] C. K. Law and H. J. Kimble, Quantum Semiclass. Opt. **44**, 2067 (1997).

[21] R. Quadt, M. Collett, and D. F. Walls, Phys. Rev. Lett. **74**, 351 (1995).

[22] A. C. Doherty *et al.,* Phys. Rev. A (to be published).

[23] D. W. Vernooy and H. J. Kimble, Phys. Rev. A **56**, 4207 (1997).